

X-ray and Raman scattering characterization of Ge/Si buried layers

R. L. Headrick

Cornell High Energy Synchrotron Source and Department of Applied and Engineering Physics, Cornell University, Ithaca, New York, 14853

J.-M. Baribeau, D. J. Lockwood, and T. E. Jackman

Institute for Microstructural Sciences, National Research Council of Canada, Ottawa, Ontario K1A 0R6, Canada

M. J. Bedzyk^{a)}

Cornell High Energy Synchrotron Source, Cornell University, Ithaca, New York, 14853

(Received 15 June 1992; accepted for publication 30 November 1992)

Germanium buried layers in (001) oriented silicon with thicknesses of 2–12 monolayers have been studied with synchrotron x-ray diffraction, x-ray reflectivity, and Raman scattering spectroscopy of visible light. Relaxation, strain, and intermixing have been observed via diffraction and intermixing is inferred from vibrational frequency shifts.

The synthesis of semiconductor layered structures with abrupt interfaces is a major goal in the development of new materials with useful electrical and optical properties. Structures such as short-period superlattices, resonant tunneling diodes, and delta-doped layers can be improved by elimination of random potential fluctuations that tend to destroy coherent effects such as tunneling, direct band gap character by zone folding,¹ and high carrier mobility.²

Current work in progress is centered on the extent of strain relaxation, and intermixing at the level of less than 1 monolayer at the Ge-Si interface.³ Synchrotron x-ray diffraction has proved to be a useful technique for measuring the strain and morphology in heterostructures.⁴ Here, we show that for buried Ge_n layers with $n \leq 5$ no relaxation and $< 3 \text{ \AA}$ vertical spreading of buried layers occur. This data is correlated with intermixing inferred from vibrational properties measured by Raman scattering spectroscopy.

The epitaxial layers were grown in a VG Semicon V80 molecular beam epitaxy system on 100-mm-diam Czochralski (001) wafers. A 1500- \AA -thick Si buffer layer was deposited at $515 \pm 25 \text{ }^\circ\text{C}$ using optimum growth procedures. The substrate was then cooled down to $385 \pm 25 \text{ }^\circ\text{C}$ and the thin epitaxial film was grown at a deposition rate of 0.2 \AA/s . The thin Ge layer was capped with $\approx 330\text{-}\text{\AA}$ -thick Si layer grown under identical conditions. Five Ge_n layers were prepared with the nominal number of Ge monolayers $n=2,3,4,5,12$, where 1 monolayer is defined as 6.78×10^{14} atoms/cm².

X-ray diffraction measurements were carried out at the Cornell High Energy Synchrotron Source (CHESS) using 1.28 \AA radiation from a two-bounce Ge(111) monochromator. Samples of 1 cm \times 1 cm area were mounted on a Huber four circle diffractometer oriented for scattering in the vertical plane. Grazing angle diffraction radial scans through the (220) reflection were carried out for each of the five samples. Specular reflectivity measurements were also performed for each sample.

The Raman spectra of the samples were recorded in a

He gas atmosphere in the quasibackscattering geometry. In this geometry first-order scattering from longitudinal phonons dominates the Raman spectrum. The samples were excited with 300 mW of 457.9 nm argon laser light, while the Raman-scattered light was dispersed with a Spex 14018 monochromator with resolution 3 cm^{-1} and detected with a cooled photomultiplier. The incident light was polarized in the plane of scattering, while the scattered-light polarization was not analyzed.

Figure 1 shows x-ray diffraction radial scans in the (110) direction through the (22L) reflection for two of the samples with $n=3$ and 12. The scans were taken with equal incident and exit angles so that $L=2d\alpha/\lambda$ ($d=5.431 \text{ \AA}$), and two scans on each sample are shown with $\alpha=0.1^\circ$ and 0.3° , where α is the grazing angle of incidence of the incident beam with the surface. The two top scans from the $n=12$ sample exhibit a sharp central peak at $H=2.00$, and a much broader peak with a maximum intensity 10%–15% of the central peak. In addition, the data at $\alpha=0.3^\circ$ shows a significant broad contribution centered at lower momentum transfer. The lower two scans in Fig. 1, from the $n=3$ sample, are dominated by the sharp peak, however, a broader contribution with maximum intensity $< 1\%$ of the central peak is also visible at $\alpha=0.3^\circ$, but not at $\alpha=0.1^\circ$.

These scans can be interpreted as scans of in-plane lattice parameter, so that layers with the same spacing as silicon contribute to the sharp peak at $H=2.00$. Fully relaxed Ge, which has a lattice parameter 4.2% larger, would contribute at $H=1.92$, however, a pseudomorphic Ge film will be indistinguishable from bulk silicon. An effect that can be observed in Fig. 1 is that of varying states of strain which produce broad features. Below we discuss these features in terms of contributions from the silicon substrate, Ge buried layer, and Si cap layer. In order to distinguish between the various layers, we make use of the limited penetration depth of x-rays at incidence angles below the critical angle for total external reflection. The inset in Fig. 1 shows the penetration depth, Λ , in units of angstroms, as a function of α . It is clear from this curve that the buried Ge layers 330 \AA below the surface may contribute to the signal at $\alpha=0.3^\circ$, but not at $\alpha=0.1^\circ$.

We first discuss two scans from the $n=12$ sample. The

^{a)}Present address: Department of Materials Science and Engineering, Northwestern University, and Materials Science Division, Argonne National Laboratory.

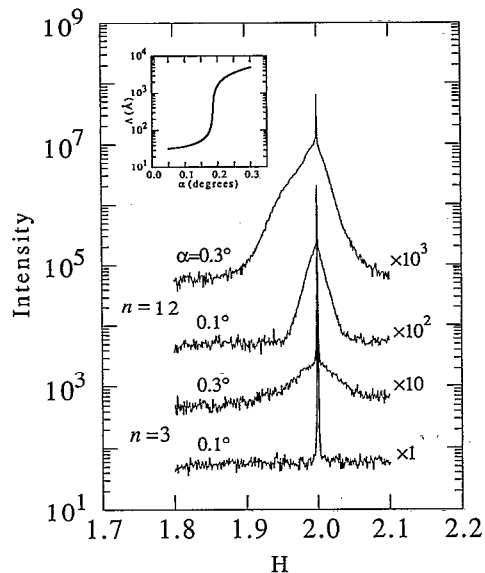


FIG. 1. X-ray diffraction radial scans through $(22L)$, with L near 0, for two different samples and two angles of incidence. The upper two scans are from the $n=12$ sample and the lower two scans are for the $n=3$ sample. Variation of the x-ray penetration depth as a function of incidence angle is shown in the inset. The penetration depth, Λ , is in units of angstroms. The data demonstrates sensitivity between the buried layer (≈ 330 Å below the silicon surface) and near-surface layers.

presence of a broad contribution near $H=1.95$ in the top scan is clear evidence for a relaxed layer, a conclusion which is consistent with many other studies of Ge growth on silicon.⁵ At the more grazing angle of incidence, the contribution from the relaxed Ge film is not visible.

Comparison of the data from the $n=3$ sample in Fig. 1 again shows sensitivity between the buried layers and near-surface layers. At the lower angle of incidence, no signal from strain or distortion can be detected. This is evidence that the cap layer is defect free within the sensitivity of the present measurement. At the higher angle of incidence, the broad peak has an intensity of 2×10^{-3} of the sharp peak. In order to distinguish the origin of the weak diffuse scattering, we make use of the energy tunability of x rays from the synchrotron source. Scattering from the Ge buried layer would vary as $|f_{\text{Ge}}|^2$, or as $|f_{\text{Ge}} - f_{\text{Si}}|^2$, where f_{Ge} and f_{Si} are the atomic scattering factors for Ge and Si.^{6,7} Scans at different energies around the Ge K edge at 11.103 keV do not reveal any variation of the diffuse scattering, confirming that the signal arises only from silicon. Thus, the signal is attributed to the silicon buffer layer or substrate. The absence of any Ge-related features for the samples with $n=2-5$ suggests that the buried layers are two-dimensional and free of significant defects.

Additional radial scans for samples with $n=0,2,5,12$ are shown in Fig. 2. For these scans, the incidence angle α was near the critical angle for total external reflection of x rays. Near the critical angle, the field intensity is increased close to the surface because of constructive interference of the incident and reflected waves, leading to an enhanced scattering from near-surface layers. For $n=12$, the central broad peak is more intense than in either of the scans

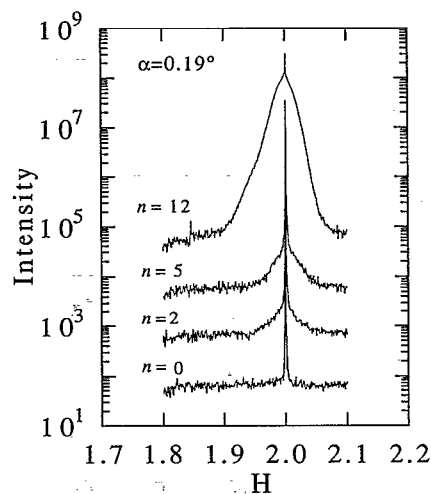


FIG. 2. Additional x-ray diffraction radial scans with the angle of incidence near the critical angle ($\alpha_c=0.19^\circ$) from four different samples. The diffuse scattering from the $n=2$ and 5 samples is attributed to strain in silicon layers. The diffuse scattering from the $n=12$ sample is from varying states of strain caused by relaxation and islanding of the Ge buried layer and by defects propagating through the cap layer. The data from the $n=0$ sample shows no detectable diffuse scattering confirming that the substrate material is relatively unstrained.

shown in Fig. 1. From this we conclude that the highest density of defects is located in the cap layer. Scans for the $n=2$ and 5 samples again show the weak diffuse peak attributed to defects in the Si substrate or buffer layer. For $n=0$, the signal is not observed, showing that the diffuse peak does not emanate from the substrate. This sample was simply a piece of the substrate material, and so, did not have any grown films of either Si or Ge.

The different Raman spectra were first processed by subtracting the dominant Raman contribution due to the Si substrate and cap from the original spectra. The results of the subtraction, shown in Fig. 3, reveal features due to the optical phonons in the Ge_n layers. Two peaks are observed near 300 and 415 cm^{-1} that are due, respectively, to

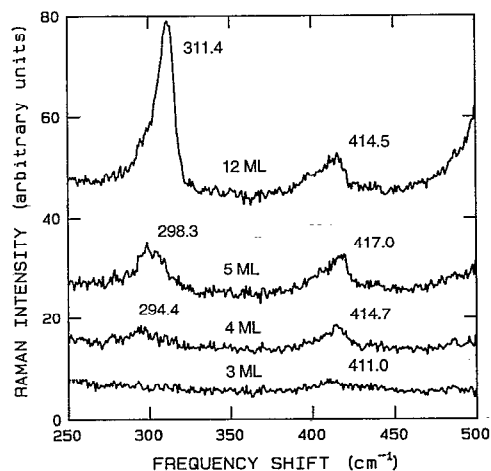


FIG. 3. Raman scattering spectra of Ge_n layers buried in Si as revealed by subtraction of the Si substrate and cap spectrum. The numbers beside the peaks are their frequencies in cm^{-1} .

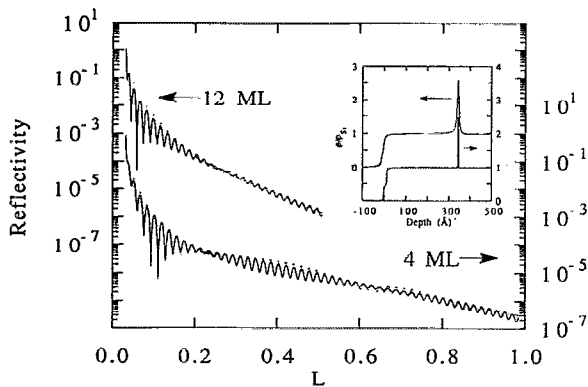


FIG. 4. X-ray reflectivity data (points) and simulations (solid lines) for $n=4$ and 12. The inset shows the electron density profiles used for the simulations.

Ge-Ge vibrations within the Ge_n layer⁸ and to the GeSi vibrations arising from Si atoms adjacent to, and within the Ge_n layer.⁹ The Ge-Ge peak exhibits considerable variation in peak frequency and intensity with n . The Raman intensity of the $n=12$ line is approximately twice as strong as would be expected from the $n=4$ and 5 results. Assuming the Raman intensity is proportional to the n value, this result implies that not all of the layers are pure Ge. An interface roughness of not more than 2 monolayers due to Si intrusion on the Ge side of each Si-Ge interface is consistent with the $n=12$, 5, and 4 Raman intensity results. This conclusion is confirmed by the apparent absence of the Ge-Ge peak in the $n=3$ spectrum, although the Si-Ge peak persists.

The presence of the Si-Ge line in the Raman spectrum is indicative of interface roughness.^{8,10} The line of similar frequency and intensity in each sample suggests that the degree of interface disorder is much the same in all four samples. Furthermore, the intensity of this line is relatively weak, indicating only a small amount of disorder.³

Figure 4 shows x-ray reflectivity curves for two of the samples. The $n=4$ curve is representative of the thinner films ($n=2-5$) which show extended interference oscillations out to $L=1$ ($Q=1.16 \text{ \AA}^{-1}$). The $n=12$ curve also exhibits extended oscillations, but they are significantly reduced in amplitude at higher momentum transfer. Reflectivity curves were calculated from:

$$I(Q) = I_F(Q) \left| \frac{1}{\rho_{\text{Si}}} \int_{-\infty}^{\infty} \frac{\partial \rho(z)}{\partial z} e^{iQz} dz \right|^2. \quad (1)$$

Here, $I_F(Q)$ is the Fresnel reflectivity for a perfectly sharp dielectric boundary between vacuum and silicon.¹¹ For a buried layer in an otherwise homogeneous semi-infinite medium, this equation for $I(Q)$ can be derived from the distorted wave Born approximation.¹² From Eq. (1) it is seen that a sharp buried layer will yield a modulation of the reflectivity with nearly a single frequency corresponding to the depth of the buried layer, while a smeared out buried layer will yield a range of frequencies that may reduce the amplitude of the modulations.

The inset in Fig. 4 shows density profiles, $\rho(z)$, derived from the two data sets. The solid lines in the figure are the calculated reflectivity from these density profiles which are seen to match the data. Smearing out of the top surface density profile and the inclusion of a thin 15–20 Å oxide layer were necessary to fit the data well. The $n=4$ profile has a density spike centered $\approx 330 \text{ \AA}$ below the top surface with perfectly sharp boundaries with the surrounding silicon. This is evidence against intermixing on the scale of the resolution of the data ($\approx 3 \text{ \AA}$). In contrast, the $n=12$ density profile has significant smearing, 5 Å at each Ge-Si interface, consistent with islanding or diffusion of the Ge film.

In this work we have applied grazing incidence x-ray diffraction to the study of very thin Ge buried layers. No strain relaxation was found in buried layers to a thickness of less than 6 monolayers. Evidence of intermixing involving no more than 2 monolayers was found by Raman scattering measurements. An upper limit for interface smearing of 3 Å FWHM was also derived from x-ray reflectivity curves. In contrast, strain relaxation, poorer crystallinity, and three-dimensional growth was found in a 12-monolayer-thick Ge buried layer. An implication of this work is that metastable Ge buried layers, up to at least 5 monolayers, can be grown in crystalline silicon with no strain relaxation, two-dimensional growth, and limited interface smearing.

This work is based upon work conducted at CHESS, supported by the National Science Foundation under Award No. DMR 90-21700.

¹S. Froyen, D. M. Wood, and A. Zunger, *Phys. Rev. B* **36**, 4547 (1987); **37**, 6893 (1988).

²C. Abstreiter, H. Brugger, T. Wolf, H. Jorke, and H. J. Herzog, *Phys. Rev. Lett.* **54**, 2441 (1985).

³J.-M. Baribeau, D. J. Lockwood, T. E. Jackman, P. Aebi, T. Tyliczszak, and A. P. Hitchcock, *Can. J. Phys.* **69**, 246 (1991).

⁴A. A. Williams, J. M. C. Thornton, J. E. Macdonald, R. G. van Silfhout, J. F. van der Veen, M. S. Finney, A. D. Johnson, and C. Norris, *Phys. Rev. B* **43**, 5001 (1991).

⁵K. Eberl and W. Wegscheider, in *Handbook on Semiconductors, Materials, Properties and Preparation*, Vol. 3, edited by S. Mahajan (Elsevier, Amsterdam, 1992).

⁶J. M. Cowley, *Diffraction Physics*, 2nd ed. (Elsevier, Amsterdam, 1981).

⁷For the case of interface roughness, the diffuse scattering is modulated according to: $I_D(Q) \propto (f_{0,\text{Ge}} + \Delta f'_{\text{Ge}} - f_{\text{Si}})^2$ as a function of energy, where $\Delta f'_{\text{Ge}}$ becomes largest and negative at 11.103 keV. The factor f_{Si} does not vary significantly over the energy range used. A Si(111) double bounce monochromator was used for the energy dependent measurements.

⁸M. W. C. Dharma-wardana, G. C. Aers, D. J. Lockwood, and J.-M. Baribeau, in *Light Scattering in Semiconductor Structures and Superlattices*, edited by D. J. Lockwood and J. F. Young (Plenum, New York, 1991), p. 81.

⁹J. Menéndez, A. Pinczuk, J. Bevk, and J. P. Mannaerts, *J. Vac. Sci. Technol. B* **6**, 1306 (1988).

¹⁰E. Molinari and A. Fasolino, *Appl. Phys. Lett.* **54**, 1220 (1989).

¹¹M. Born and E. Wolf, *Principles of Optics*, 6th ed. (Pergamon, Oxford, 1989), p. 40.

¹²S. K. Sinha, E. B. Sirota, S. Garoff, and H. B. Stanley, *Phys. Rev. B* **38**, 2297 (1988).